

Biom mineralization of calcium carbonate by adding aspartic acid and lysozyme

Sung Moon Song and In Ho Kim[†]

Department of Chemical Engineering, Chungnam National University, 220, Gung-dong, Yuseong-gu, Daejeon 305-764, Korea
(Received 24 December 2010 • accepted 27 January 2011)

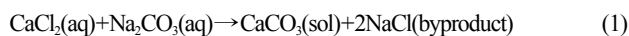
Abstract—Calcium carbonate is one of the most abundant materials present in nature. Crystal structures of CaCO₃ become three polymorphic modifications, namely calcite, aragonite and vaterite. Polymorphic modifications are mediated by adding aspartic acid (Asp) and lysozyme. Lysozyme, which is a major component of egg white proteins, has influenced the calcification of avian eggshells. The influence of Asp and lysozyme on the crystallization of CaCO₃ was investigated by adding these additives and calcium chloride solution into sodium carbonate solution in a crystallization vessel. CaCO₃ crystals were analyzed by X-ray diffraction (XRD), field emission scanning electron microscopy (FE-SEM) and Fourier transform infrared spectrometry (FT-IR). XRD was used to select the intensities and crystal structure of specific calcium carbonate. SEM was employed for the analysis of the morphology of the precipitation and particle size. Two kinds of crystals were identified by FT-IR spectrum. Hexagonal crystals of vaterite were affected by the Asp in the crystallization solution. However, rhombohedral crystals of calcite by lysozyme were formed without any sign of vaterite.

Key words: Calcium Carbonate, Aspartic Acid, Lysozyme

INTRODUCTION

CaCO₃ crystal is essential to form the frame of an organism and has contributed to synthesis of nanomaterials. In biom mineralization, calcium carbonate (CaCO₃) is one of the most abundant mineral resources formed in the natural environment. CaCO₃ has increasingly attracted interest and industrial demand has increased for several years on account of physical and chemical properties of CaCO₃. Therefore, crystallization of calcium carbonate was extensively studied as it is widely used in the paper, paint, rubber and biomedical application [1]. The application of calcium carbonate particles is determined by several factors, such as particle morphology, specific surface area, particle size, particle size distribution [2]. Calcium carbonate exhibits three polymorphic modifications (rhombohedral calcite, needlelike aragonite and spherical vaterite) [1]. Crystal properties can be controlled by modifying the reaction medium using surfactants, suspensions, additives and precipitation conditions such as pH [3] and temperature. Calcite is usually formed at a high solution pH and low temperature, while vaterite and aragonite are formed at a low solution pH and high temperature. They are transformed to stable calcite since vaterite is unstable crystal morphology [4-6]. The ACC (amorphous calcium carbonate) forms in the initial stage of calcium carbonate reaction, and it is transformed into vaterite, aragonite and calcite [7-10].

The gas-liquid reaction of CaCO₃ is that CO₂ gas is absorbed into calcium hydroxide solution. CaCl₂-Na₂CO₃ represents liquid-liquid reaction. The liquid-liquid reaction for CaCO₃ crystallization makes both CaCO₃ crystals and NaCl byproduct as Eq. (1)



[†]To whom correspondence should be addressed.
E-mail: ihkim@cnu.ac.kr

This is because the reaction easily controls saturation concentration in solution and produces various morphologies of CaCO₃ crystallization. It is easy to produce biom minerals from CaCO₃ crystallization reaction by a liquid-liquid reaction with organic materials.

Previous reports showed that the polymorph of calcium carbonate is dependent on the operating conditions of the crystallization, such as supersaturation [11], solution composition [12], pH [10], temperature [14], and presence of additives [15,16]. Biom mineralization produces biom mineral with good property by adding amino acid to CaCO₃ [17]. The outside shell of shellfish is organized by mainly calcite and CaCO₃ layer structure. This layer structure's fracture toughness is thousands times as strong as that of simple CaCO₃ crystals, while aragonite forms inside layer structure.

There are many studies of biopolymer which affect polymorph formation. Henderson et al. [18] discovered that glycine and alanine are used for crystal reaction of vaterite. Many proteins such as ansocalcin, lysozyme and lithostathine which affect calcium carbonate polymorph have been studied [19]. The studies of calcium carbonate polymorph using polysaccharide were presented by Xiao et al. and Arias and Fernandez [20]. Study of polymorph using nucleic acid was reported by Lukeman et al. [21].

The aim of the present work is to study the role of Asp and lysozyme on the precipitation of calcium carbonate. Morphology of CaCO₃ crystals is affected by additives such as aspartic acid (Asp) or lysozyme into calcium chloride and sodium carbonate solution. Lysozyme is a major component of egg white proteins and plentiful in eggshell membranes, which seems to be a modulator for CaCO₃ crystallization. Analytical investigations of CaCO₃ by FE-SEM, XRD and FT-IR were performed, as well as to discuss the mechanism. FE-SEM was used in order to analyze morphology and crystal size. XRD was used to measure peak intensities and the presence of CaCO₃ polymorph. Crystal morphology change with reaction time was identified with measured peak areas of XRD pattern and

FT-IR data.

EXPERIMENTAL

Anhydrous calcium chloride (CaCl_2) (purity $\geq 99.0\%$) and sodium carbonate (Na_2CO_3) (purity $\geq 99.0\%$) were purchased from Oriental Chemical Inc. (Korea) and Duksan Pharmaceutical Co. Ltd. (Korea), respectively. D, L-aspartic acids were purchased from Fluka (USA). Lysozyme from egg white (purity $> 95\%$, MW = 14.3 kDa) was ob-

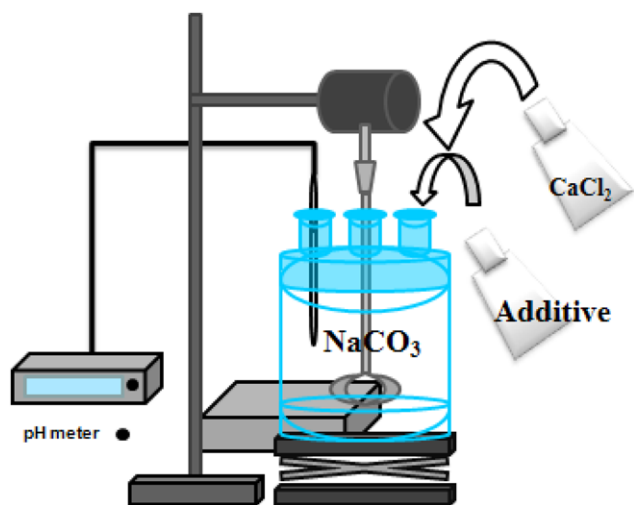


Fig. 1. Schematic diagram of experimental apparatus for biomineralization of calcium carbonate.

tained from Sigma (USA). Distilled water was used to prepare aqueous solutions of CaCl_2 and Na_2CO_3 just before crystallization experiment.

For the crystallization of CaCO_3 in the absence and the presence of Asp and lysozyme, the liquid-liquid reaction was applied under ambient laboratory conditions. This reaction is illustrated in Fig. 1. In a typical process, experiments were performed in a Pyrex vessel at 25°C , and the working volume was 1.0 L. Control crystallization solutions were prepared by mixing equal volumes (500 mL) of 50 mM calcium chloride (CaCl_2) and 50 mM sodium carbonate (Na_2CO_3). To understand the influence of additives, a crystallization solution was prepared with a 0.05 M aspartic acid (Asp) solution or 0.5 g/L, 1 g/L lysozyme. The stirring speed was controlled around 300 rpm. Samples were collected as 50 mL at various time intervals (5, 15, 120, 600 min). Samples of the product suspension were taken intermittently during reaction, and filtered immediately using a micromembrane filter with a $0.45\ \mu\text{m}$ pore diameter. And then filtered samples were dried at 50°C for 24 h. Details of experiments are given in Refs [22,23].

After being dried, the solid residues were characterized by SEM, on a JEOL JSM-7000F microscope for their crystal morphology and by multipurpose XRD for calculating the ratio of calcite to vaterite of CaCO_3 . XRD (Rigaku D/MAX-2200 Ultima/PC, Japan) measurements were conducted using $\text{Cu K}\alpha$ radiation (40 keV, 30 mA) to identify the composition of the crystals. The scanning step was 0.02° and 2θ ranges from 10° to 80° . In addition, infrared spectra were recorded with FT-IR. The dried CaCO_3 samples were ground with anhydrous KBr to produce pellets to facilitate the FT-IR characterization in the region of $4,000\text{--}600\ \text{cm}^{-1}$ using a Shimadzu spec-

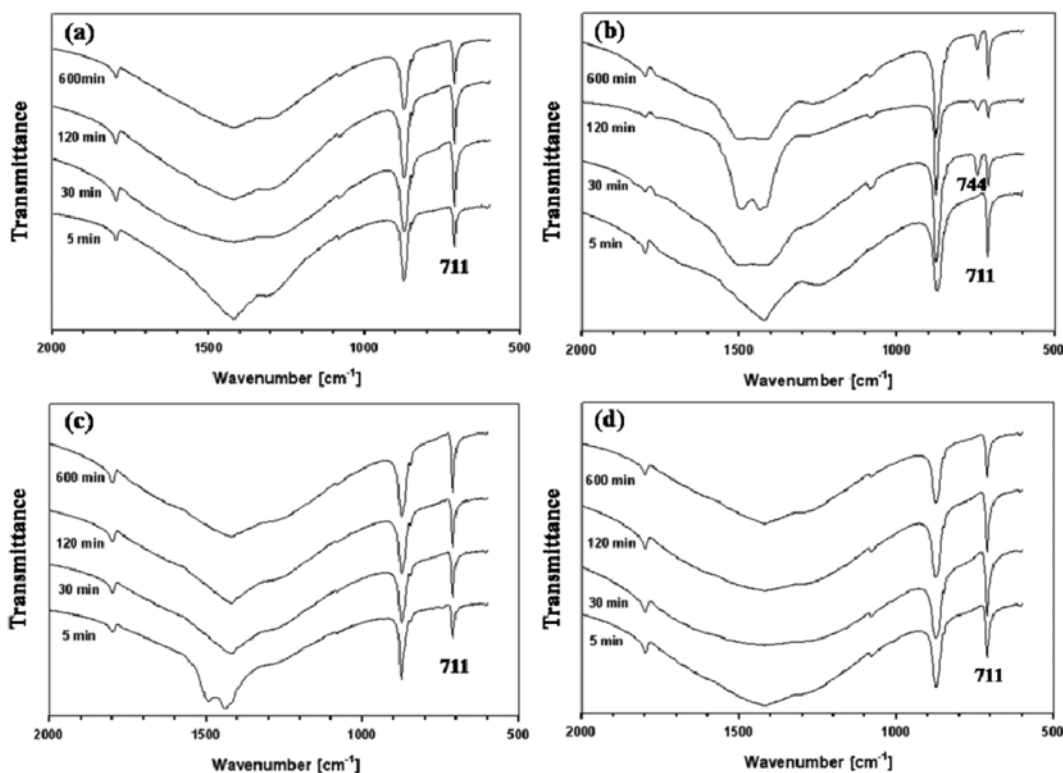


Fig. 2. Fourier transform infrared (FT-IR) spectra of CaCO_3 formed; (a) without additive (the control experiment), (b) with 0.05 M Asp, (c) with 0.5 g/L lysozyme, (d) with 1.0 g/L lysozyme. Note that the 711 and $744\ \text{cm}^{-1}$ are the peaks of calcite and vaterite, respectively.

trophotometer (Rrestoge-21). From the data of the Joint Committee on Powder Diffraction Standards (JCPDS), it was compared with actual XRD data.

RESULTS AND DISCUSSION

The decomposition of Na_2CO_3 led to the ion of Na^+ and CO_3^{2-} , both of which subsequently diffused into the CaCl_2 solution. The formed Cl^- ions were neutralized by Na^+ ions. The formation of CaCO_3 precipitates caused the excess of Cl^- ions that were neutralized by Na^+ .

Similar experiments were carried out with and without additives to examine its effect on the nucleation and phase transformation of calcium carbonate crystals. The determination of the polymorph of CaCO_3 has mainly been conducted by using FT-IR. FT-IR spectra shown in Fig. 2(a) were obtained from the samples at different time intervals without any additive (control). Between the characteristic IR peaks for calcite (711 , 875 and $1,087\text{ cm}^{-1}$) and vaterite (744 , 875 and $1,478\text{ cm}^{-1}$), the peaks at 711 and 744 cm^{-1} were used to distinguish calcite and vaterite, respectively. These IR peaks are characteristic of the calcite at 711 cm^{-1} in Fig. 2(a). In comparison, FT-IR spectra obtained from CaCO_3 precipitates formed in the presence of 0.05 M Asp are shown in Fig. 2(b). In the precipitation process of CaCO_3 , calcite was first formed. With the incubation time increasing to 30 min , ACC was transformed into a mixture of vaterite and calcite. From 30 min , the peak of vaterite at 744 cm^{-1} appeared, and then the peak of vaterite decreased. Because vaterite is the most unstable crystalline polymorph, it is transformed into the most stable calcite. So the peak of calcite increased with decreasing the peak of vaterite. Figs. 2(c) and 2(d) show the FT-IR spectra with 0.5 g/L

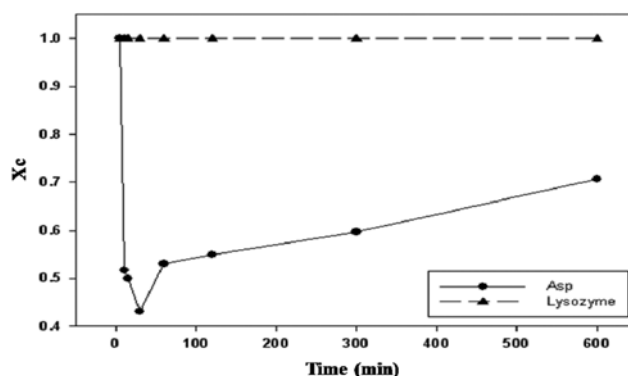


Fig. 3. Fraction of calcite calculated by measuring the weight ratio of calcite and vaterite peaks in FT-IR spectra; X_c =fraction of calcite, X_v =fraction of vaterite, $X_c=1-X_v$.

and 1 g/L lysozyme, respectively. There were only the peaks of calcite, because lysozyme restrained the vaterite from being produced. In addition, with increasing the concentration of lysozyme from 0.5 g/L to 1.0 g/L , the transmittance of calcite peaks increased.

Fig. 3 illustrates that the fraction of weight ratio of calcite changes with Asp or lysozyme in FT-IR. Eq. (2) explains the calculation method by FT-IR spectral data in which calcite and vaterite peak area are obtained by measuring the peak area. The ratio X_c was calculated by Eq. (2). X_c means the percentage of calcite and X_v in Eq. (3) equals to 1 minus X_c .

$$X_c = \frac{\text{Calcite peak area}}{\text{Calcite} + \text{Vaterite peak area}} \quad (2)$$

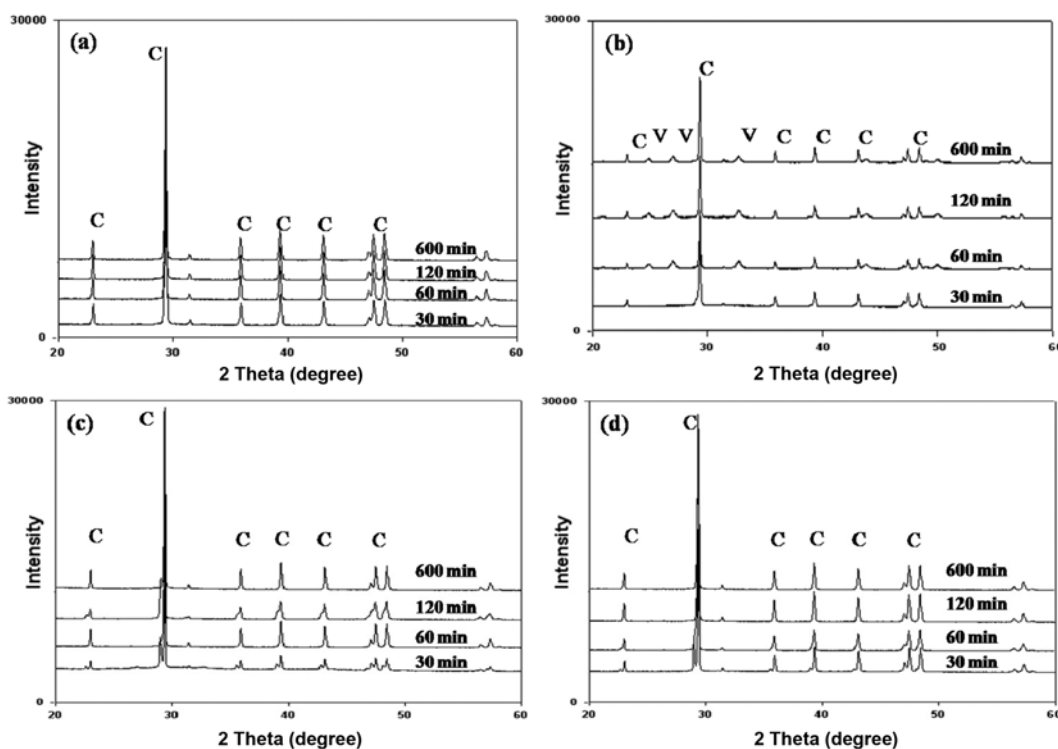


Fig. 4. X-ray diffraction (XRD) pattern of CaCO_3 precipitation (a) without additive (the control experiment), (b) with 0.05 M Asp , (c) with 0.5 g/L lysozyme, (d) with 1.0 g/L lysozyme; C=calcite, V=vaterite.

$$X_v = 1 - X_c \quad (3)$$

In the early phase, X_c rapidly decreased with Asp until 30 min. It means that vaterite was produced rather than calcite. After that, vaterite transforms to calcite X_c increases. This is because vaterite is unstable morphology among the CaCO_3 crystal. With the time

increasing, X_c was constantly increased. However, X_c was dominant with lysozyme. We expect that Asp causes vaterite morphology and lysozyme induces calcite morphology.

With the aim to further characterize the phase composition of crystals, X-ray diffraction (XRD) measurement was performed for the collected precipitates. Fig. 4(a) shows the XRD pattern for the

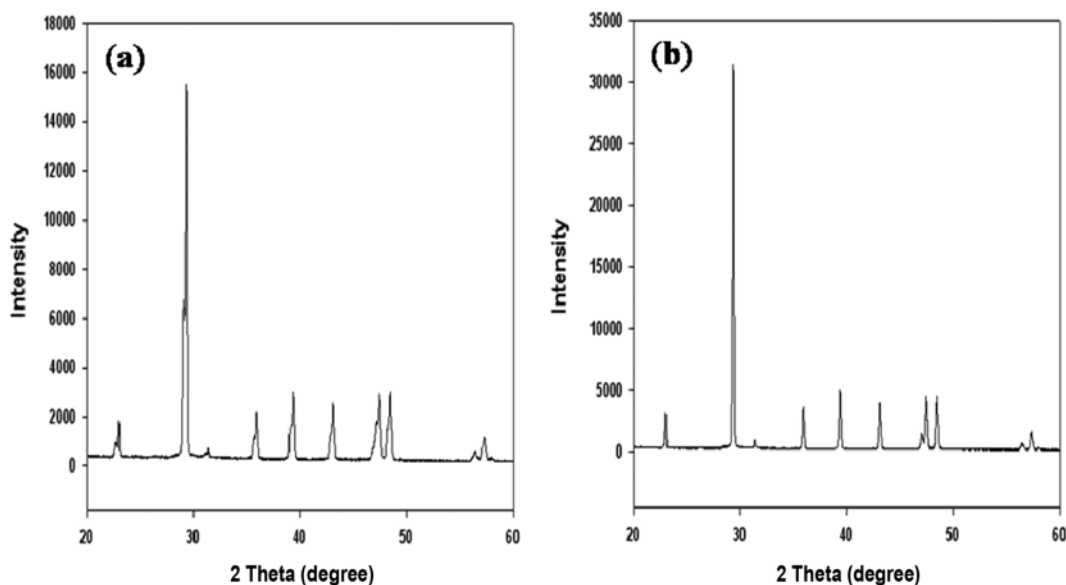


Fig. 5. X-ray diffraction (XRD) pattern of CaCO_3 precipitation collected at 120 min (a) with 0.5 g/L lysozyme, (b) 1.0 g/L lysozyme.

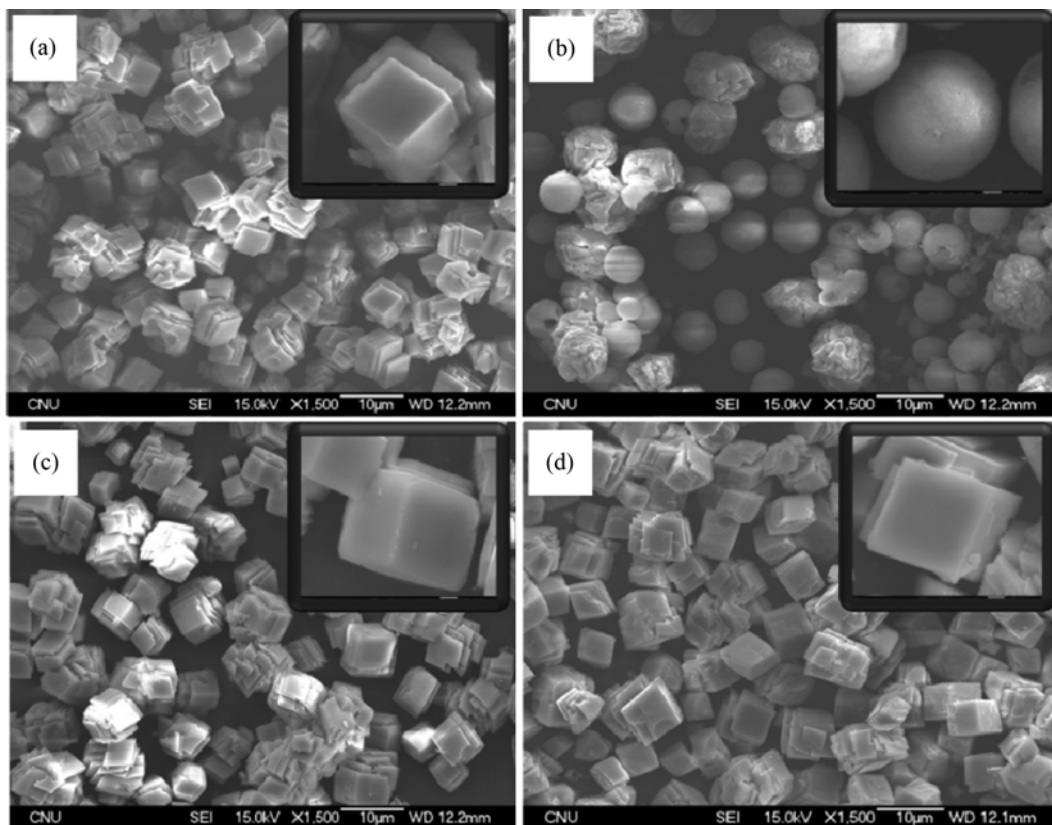


Fig. 6. SEM images of calcium carbonate crystal at 600 min; (a) without additive, (b) in the presence of 0.05 M Asp, (c) 0.5 g/L lysozyme (d) 1 g/L lysozyme.

collected precipitates without any additive. It is obvious that the crystalline phase mostly consists of calcite phase. Fig. 4(b) shows the XRD pattern with 0.05 M Asp in the presence of 0.05 M Asp; the mineral phase is composed of calcite and vaterite crystalline phase. From 120 min, intensity of XRD peaks decreased, because the unstable vaterite was transformed to the stable calcite. Figs. 4(c) and (d) show the XRD pattern with lysozyme. The mineral phase is exclusively composed of calcite crystalline phase, and no other crystalline phase was detectable. These results completely correspond with those gained from the FT-IR characterization. Moreover, it was surveyed that the concentration of lysozyme influences the crystalline phases of CaCO₃ (Fig. 5). The peak intensity of calcite was proportional to the concentration of lysozyme.

SEM is capable of revealing the morphological structure and orientation of crystals. SEM images of the CaCO₃ precipitates collected with or without additives in Fig. 6. Fig. 6(b) show the morphology of spherical vaterite crystal in the presence of 0.05 M Asp. In addition, a phase transition is also observed with Asp, since vaterite crystals coexisted with calcite crystals. As the concentration of lysozyme was increased from 0.5 g/L to 1.0 g/L, only rhombohedral calcite crystals were observed. In addition, the morphological modification of rhombohedral calcite morphology became clearer (Fig. 6(d)). The morphology of rhombohedral calcite depends on the concentration of lysozyme.

CONCLUSIONS

An experiment was conducted to control the polymorphism of calcium carbonate crystals by adding additives such as aspartic acid and lysozyme. To compare the influence of the additive, a control experiment was first performed and Asp or lysozyme was added into the experiment. In the presence of Asp, spherical vaterite crystals were produced; however, vaterite was transformed to calcite soon. The reason is that vaterite is unstable morphology and calcite is the most stable morphology. In the presence of lysozyme, there were only the peaks of calcite, because lysozyme restrained vaterite formation. Moreover, the concentration of lysozyme influences the crystalline phases of CaCO₃. The amount of calcite was proportional to the concentration of lysozyme.

ACKNOWLEDGEMENT

This research was supported by Korea Research Foundation Grant. The authors greatly appreciate the support for allowing the present

work.

REFERENCES

1. C. Shivkumara, P. Singh, A. Gupta and M. S. Hegade, *Mater. Res. Bull.*, **41**, 1455 (2006).
2. K. Tamura and H. Tsuge, *Chem. Eng. Sci.*, **61**, 5818 (2006).
3. X. Sun, Y. Zhou, J. Ren, F. Cui and H. Li, *Appl. Phys.*, **7**, 75 (2007).
4. S. Bentov, S. Weil, L. Glazer and A. Berman, *J. Struct. Biol.*, **171**(2), 207 (2010).
5. L. Gago-Duport, M. J. I. Briones, J. B. Rodriguez and B. Covelo, *J. Struct. Biol.*, **162**(3), 422 (2008).
6. M. Faatz, F. Grohn and G. Wegner, *Mater. Sci. Eng.*, **25**(2), 153 (2005).
7. R. Beck and J. Andreassen, *Cryst. Growth*, **312**(15), 2226 (2010).
8. W. M. Jung, S. H. Kang, W. S. Kim and C. K. Choi, *Chem. Eng. Sci.*, **55**(4), 733 (2000).
9. S. H. Kang, I. Hirasawa, W. S. Kim and C. K. Choi, *J. Colloid Interface Sci.*, **288**(2), 496 (2005).
10. H. Wei, Q. Shen, T. Zhao, D. Wang and D. Xu., *Cryst. Growth*, **260**(3), 545 (2004).
11. J. Kawano, N. Shimobayashi, M. Kitamura, K. Shinoda and N. Aikawa, *J. Cryst. Growth*, **237**, 419 (2002).
12. Y. Li, T. Wiliama and K. C. Tam, *Mater. Res. Bull.*, **42**(5), 820 (2007).
13. G. Hadiko, Y. S. Han, M. Fuji and M. Takahashi, *Mater. Lett.*, **59**(19), 25192 (2005).
14. Y. S. Han, G. Hadiko, M. Fuji and M. Takahashi, *J. Cryst. Growth*, **289**(1), 269 (2006).
15. D. Zhao, T. Zhu, F. Li, Q. Ruan, S. Zhang, L. Zhang and D. Xu, *Mater. Res. Bull.*, **45**(1), 80 (2010).
16. J. Aizenberg, S. Albeck, S. Weiner and L. Addadi, *J. Cryst. Growth*, **142**(1), 156 (1994).
17. H. Wentao and F. Qingling, *Mater. Sci. Eng.*, **26**(4), 644. (2006).
18. G. E. Henderson and K. M. McGrath, *J. Cryst. Growth*, **244**(3), 369 (2002).
19. Y. Hu, Y. Ma, Y. Zhou, F. Nie, X. Duan and C. Pei, *J. Cryst. Growth*, **321**(10), 1741 (2010).
20. G. Frenandez and E. Castro, *J. Food Eng.*, **92**(1), 112 (2009).
21. P. S. Lukeman, W. B. Sherman, C. Micheel, A. P. Alivisatos and N. C. Seeman, *Biophys. J.*, **95**(1), 3340 (2008).
22. J. H. Kim, J. M. Kim, W. S. Kim and I. H. Kim, *Korean Chem. Eng. Res.*, **47**(2), 213 (2009).
23. J. H. Kim, S. M. Song, J. M. Kim, W. S. Kim and I. H. Kim, *Korean J. Chem. Eng.*, **27**(5), 1535 (2010).